Ambiente & Água - An Interdisciplinary Journal of Applied Science
ISSN 1980-993X – doi:10.4136/1980-993X
www.ambi-agua.net
E-mail: ambi.agua@gmail.com

Effect of lithological and geotechnical characteristics on the generation of debris flows in the arid basin of Mirave, Peru

ARTICLES doi:10.4136/ambi-agua.2785

Received: 28 Aug. 2021; Accepted: 09 Mar. 2022

Julio César Bizarreta Ortega[1]; Marko Antonio Lopez Bendezu[2]; Alexandre Almeida Del Savio[2*]; Fausto Alfredo Canales[3]

[1]Instituto Latino-Americano de Tecnologia, Infraestrutura e Território. Universidade Federal da Integração Latino-Americana, Avenida Silvio Américo Sasdelli, n° 1842, CEP: 85866-000, Foz do Iguaçu, PR, Brazil. E-mail: jcbizarreta@gmail.com
[2]Instituto de Investigación Científica. Department of Civil Engineering. Universidad de Lima, Avenida Javier Prado Este, n° 4600, 15023, Santiago de Surco, Lima, Peru. E-mail: mlopezb@ulima.edu.pe
[3]Department of Civil and Environmental. Universidad de la Costa, Calle 58#55-66, 080002, Barranquilla, Atlántico, Colombia. E-mail: fcanales@cuc.edu.co
[*]Corresponding author. E-mail: delsavio@gmail.com

ABSTRACT

Studies concerning the debris flows in mountain areas are relevant because of their potential negative effects on the human communities and infrastructure in their areas of influence. To advance the understanding of the theoretical basis, this study qualitatively analyzes the effect of lithological characteristics and soil type on the generation of debris flows in the arid basin of Mirave, in southern Peru, as a consequence of extensive rainfall. Two debris flow events are evaluated, which occurred in the studied area in March 2015 and February 2019. The method used to achieve the objective combines the use of satellite images, field data collection, and lab tests results to estimate the relative importance of the abovementioned characteristics in the generation of debris flows. The results suggest that the poor presence of clay and the predominance of sandy-loamy structured soils in the Mirave Basin make them unstable when erosion occurs. In addition, the features of broken down materials generated from residual and colluvial soils in the primary area of study are one of the main causes of debris flows in the region.

Keywords: arid basin, debris flows, geotechnical characteristics, lithology.

Efeito das características litológicas e geotécnicas na geração de fluxos de detritos na bacia árida de Mirave, Peru

RESUMO

A relevância dos estudos sobre os fluxos de detritos em áreas montanhosas se deve aos seus efeitos negativos potenciais sobre as comunidades humanas e a infraestrutura em suas áreas de influência. Visando contribuir para o avanço no entendimento do embasamento teórico, o presente estudo analisa qualitativamente o efeito das características litológicas e do tipo de solo na geração de fluxos de entulho na bacia árida de Mirave, no sul do Peru, em decorrência de chuvas intensas. São avaliados dois eventos de fluxo de detritos, que ocorreram na área estudada em março de 2015 e fevereiro de 2019. O método utilizado para atingir o objetivo

combina o uso de imagens de satélite, coleta de dados de campo e resultados de testes de laboratório para estimar a importância relativa do características supracitadas na geração de fluxos de detritos. Os resultados sugerem que a fraca presença de argila e a predominância de solos estruturados arenoso-argiloso na bacia do Mirave os tornam instáveis quando ocorre a erosão. Além disso, as características dos materiais degradados gerados a partir de solos residuais e coluviais na área primária de estudo são uma das principais causas dos fluxos de detritos na região.

Palavras-chave: bacia árida, características geotécnicas, fluxos de detritos, litologia.

1. INTRODUCTION

Based on their magnitude and frequency, debris landslides have been studied around the world in relation to the potential negative impacts on the human communities in their area of influence. Debris flows and rockfalls are some of the main geomorphological processes in the Andes, particularly in the arid Andean zones (Moreiras, 2006). When such flows get activated in basins, they follow the path of natural drainage; those that run along natural channels (Chen *et al.*, 2009) are referred to as channeled debris flow. Usually, an initiating or generating zone, a flow transportation or conducting zone, and a deposition zone are present in a debris flow event (Imaizumi *et al.*, 2016). The initiation zones of debris flow due to extensive precipitations are mainly affected by availability, type, and classification of soil, lithology, current strength, the slope, soil usage and cover, and the density of previous events (Esper Angillieri *et al.*, 2020; Meyer *et al.*, 2014). Lithology studies and soils are fundamental for understanding the types of mechanisms linked to an event, as well as to evaluate the zones that are prone to the initiation of debris flow. This is because the types of rocks and soil play a key role in the formation and buildup of surface unconsolidated sediments, which induce debris flows (Di *et al.*, 2019). In general, the literature states that the lithology and the types of soils are critical in the occurrence of this phenomenon (Cannon and Reneau, 2000; Esper Angillieri, 2020; Ding *et al.*, 2020). The debris flow is mainly generated in steep slope zones ranging from 20° to 45°, initiated by surface breakdowns of slopes in the heads or hillside slopes of gullies, or sometimes in the bed of steep drainage channels, during events of extreme runoff (Hungr, 2005).

This research work is focused on the arid basin located in the town of Mirave, in the Tacna region of the Sechura–Atacama Desert. This desert rests on the western side of the Andes Range and the Pacific Ocean. This area has a lot of arid basins along which the dry rivers run; these are local rivers exhibiting the debris flow, and these rivers may remain dry for long periods of time, normally measured in years. When such basins become active, they are generally manifested as an event of debris flow. The mechanisms and the location of areas prone to the generation of debris flow in these regions are barely studied, as well as the effect of lithological aspects and soil characteristics.

Debris flows are expected in many Peruvian locations due to steep slopes, high mountains, extremely arid western foothills with rocks and soils susceptible to removal by rainwater. However, debris flows have only been reported in Mirave for 2015 and 2019, and according to the elderly residents, in 1927. The paper describes the lithological and geotechnical characteristics of the Mirave Basin and complements the work by Del Savio *et al.* (2019) by discussing the effect of these characteristics, thus improving the understanding of the debris flow generation in this region.

By using the finite differences method provided by the commercial software FLO-2D, Del Savio *et al.* (2019) simulated the debris flow that occurred in 2019 in the same region. This software applies a numerical integration of flow motion and conservation equations to simulate the debris movement of a 2D scenario (Chang *et al.*, 2020). The numerical simulation does not entirely reproduce the physical phenomenon but uses the liquid hydrographs of flow for

different periods of time to determine the affected area and the zones of debris deposition. Del Savio *et al.* (2019) provide the parameters to numerically simulate a model in FLO-2D, including the debris flow rates, hydrographs, and volume of the debris flow in the four micro-ravines of the Mirave Basin; and the rheological parameters of the debris flow. However, one of its limitations is that it does not consider the characteristics of surface lithology of the micro basin. In this context, this research aims to qualitatively evaluate the effect of lithological characteristics and soil types in the generation of debris flow in the Mirave Basin, which is part of the Sechura–Atacama Desert, in southern Peru.

By focusing on the Mirave Basin area, this research contributes to the literature related to debris flows in hyperarid environments. In South America, similar case studies on debris flow in the Andean region include the paper by Melendez *et al.* (2021), who applied a TETIS hydrological simulation model on the Lurin River Basin on the arid coast of Peru. The information for the hydrological model calibration was available; however, geotechnical and lithological data was not included in the modeling, missing some accuracy related to the desertic conditions of the region. Lara *et al.* (2018) carried out a geomorphological study to determine the characteristics of the arid basin of the La Ciénaga River in Argentina. They found that the basin is in an active tectonic environment and that all the sub-basins analyzed share an elongated shape, which allows a rapid concentration of water that intensifies the power of flash floods, very similar to the Mirave Sub-basins. Besides these examples, the review paper by Moreiras *et al.* (2021) compiled research related to this type of event in the semiarid Central Andean region, highlighting the importance of improving the knowledge on the subject and implementing preventive measures to protect the Andean communities.

2. METHODS

2.1. Location and Characterization of the Study Area

Figure 1 shows the location of the Tacna region in the south of Peru and the red lines outline the Mirave Basin, which belongs to the Ilabaya District. The town of Mirave lies at an average altitude of 1100 masl, at the micro basin mouth of the Mirave ravine (Medina Allca and Luque Poma, 2016), at the UTM coordinate: 8066400 North; 334400 East; datum WGS 84, and Zone 19S. The inhabitants of the town (approximately 800 people) did not want to be relocated despite knowing that they inhabit a high-risk geological area due to mass movement (Ilabaya, 2016).

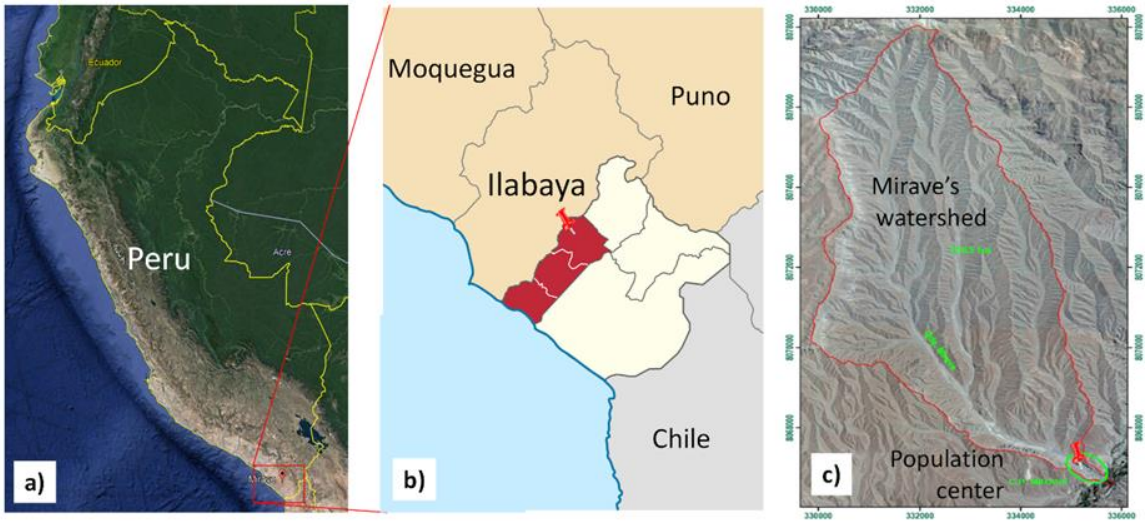

Figure 1. a) Location of the Tacna region in Peru; b) Map of Tacna where the District of Ilabaya is situated; c) Basin and town of Mirave.

The sub-basin is characterized by the erosion of sediments known as the Moquegua formation, corresponding to the period starting during the Eocene (~50 mya) up to the Pliocene (~4 mya) (Decou *et al.*, 2013), and a small part of the Toquepala group from the Early Cretaceous, called the Paralanque formation (Bellido Bravo, 1979).

Guerrero *et al.* (2013) classified the climates of the Sechura–Atacama Desert as hyperarid, arid, and semiarid climates. The debris flows occurring in these regions generally run on natural channels that remain dry most of the year. The nearest meteorological station is the Ilabaya station, situated 5 km from the high sub-basin of Mirave, which lies at an altitude of 1375 masl. According to the Servicio Nacional de Meteorología e Hidrología del Peru (SENAMHI, 2021) the rainfalls only occur in the summer months (December, January, February, and March). Taking some recent years as reference, the climate classification applied by Guerrero *et al.* (2013) would characterize the year 2016 as a hyper arid climate year (i.e., with a precipitation $\leq$ 5 mm/year), the years 2017 and 2018 as arid climate years (5 < precipitation $\leq$ 50 mm/year), and the years 2015 and 2019 as semi arid climate years (50 < annual precipitation < 250 mm/year). The latter ones are particularly interesting for our study because they coincide with the occurrence of debris flows. The sudden rains in arid areas such as Mirave may range from moderate to heavy, which may trigger debris flows and floods, according to the findings of Stolle *et al.* (2015) and Houston (2006) for arid zones. Considering the effect of other extreme climate events, the 2015 event in Mirave was not associated with the El Niño phenomenon, whereas the 2019 event coincided with the coastal El Niño phenomenon.

The occurrence of debris flows in the Mirave area is associated with exceptional rainfall, and they are classified into old and recent debris flows. The origin of the deposits corresponds to ancient debris and mudflows from the sedimentary outcrops of the Lower Moquegua Formation. Mostly during January, atmospheric patterns related to the Southern Hemisphere's summer season modulate the spatial distribution of rainfall, air temperatures, humidity, and other variables on the South American continent (SENAMHI, 2021). In this season, the Intertropical Convergence Zone moves to the south near the equator, the presence of the South Atlantic Convergence Zone and an anticyclonic circulation pattern of high-altitude wind flows (12 km) known as the High from Bolivia, is activated. These systems are the main drivers of convective rainfall in large parts of Peru and facilitate the development of storms (Medina Allca and Luque Poma, 2016).

The Ilabaya station recorded an 8-mm precipitation on March 26, 2015, a date when the debris flow occurred in Mirave. On previous days, from March 22, 2015, total daily rainfalls of 1, 8, 2, and 4 mm were recorded. According to the Instituto Nacional de Defensa Civil (INDECI, 2019) and the SENAMHI (2021), this event destroyed 60 houses and the street pavement, but no deaths were reported. Notably, retention dams were built before the event along the stream's course. These works reduced the effects of the debris flows, as described by Del Savio *et al.* (2019). Figure 2 shows the location of the dams built in the studied micro basin.

The event of February 8, 2019 had a greater magnitude than that of 2015 and was triggered by a rainfall of approximately 35 mm in the upper Mirave Basin, as recorded at the Ilabaya station. This debris flow occurred two days after a minor rainfall (SENAMHI, 2021). According to the data from government agencies (INDECI, 2019), this event resulted in two deaths, affecting 905 people and destroying 76 houses, among other damages.

From the field study conducted after the events, the occurrence of these disasters can be explained mainly because the town center is located in the alluvial range of the sub-basin, i.e., the natural drainage area of the debris that flows into the river is occupied by houses and other structures. The main identified factors that favored the debris flow in Mirave are (i) slopes with current erosion processes (gullies) that feed material into the stream channel; (ii) slopes that range from 25° to 70° that facilitate erosion of soil cover and rock; iii) unconsolidated conglomerate rock with a sandy-loamy matrix that is easily eroded by rainfall, accelerating the

formation of loose material and contributing to the sediment load toward the gully; and iv) the absence of vegetation cover, which allows for a rapid acceleration of slope erosion.

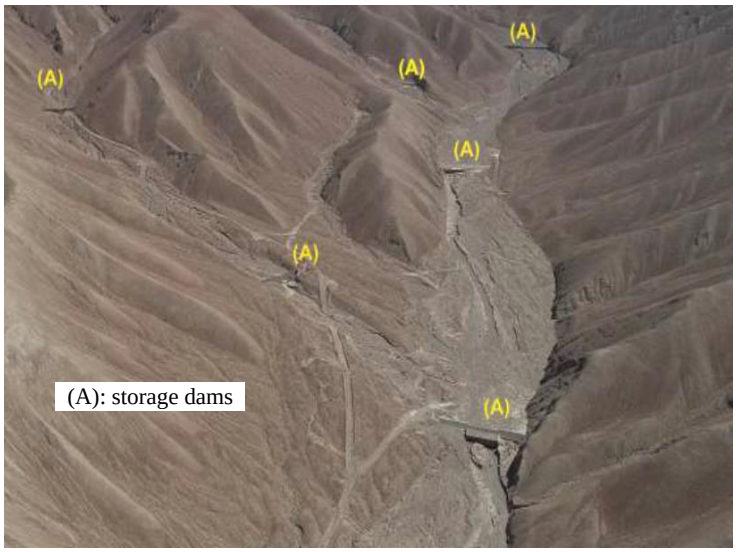

Figure 2. Location of sediment storage dams.

The retaining dams or energy dissipating walls were filled by the materials transported by the debris flows. While passing through the urban area, they first moved through the stadium (Figure 3a) having 10-m high outer walls, which were completely buried, as shown in Figure 3b. The mass of the flow destroyed part of the walls and reached the stands and sport fields. Throughout its entire course, the flow destroyed the houses in its path.

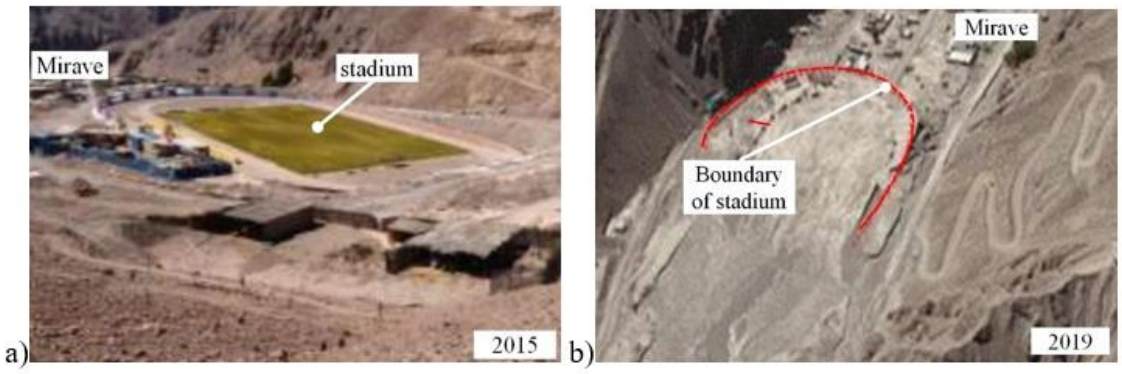

Figure 3. A debris flow occurred on a) March 26th, 2015, and b) February 8th, 2019.

2.2. Lithology and Soils in Mirave's Sub-Basin

The geological analysis of the study area was developed based on the geological map of the Moquegua quadrangle (Martinez and Zuloaga, 2000), the interpretation of aerial photographs (Del Savio *et al.*, 2019), Google Earth satellite images, and their own in-situ observations.

Observations were made throughout the Mirave drainage basin, mainly in the upper basin and sites near the watershed, to qualitatively determine the relative importance of lithology on the onset of debris flows due to rainfall. These observation rounds included twelve soil sample collection points and covered the type and quality of rock masses, soils resulting from weathering and transport, vegetation, slope, and the presence of erosional features. Google Earth satellite images were used in inaccessible or unexplored areas. Based on the aforementioned data, the lithological map was prepared, as shown in Figure 4, which in addition to the lithological units, shows the recent alluvial and storm-water deposits resulting from debris

flow, located from the drainage areas to the alluvial fan that reaches the Salado River.

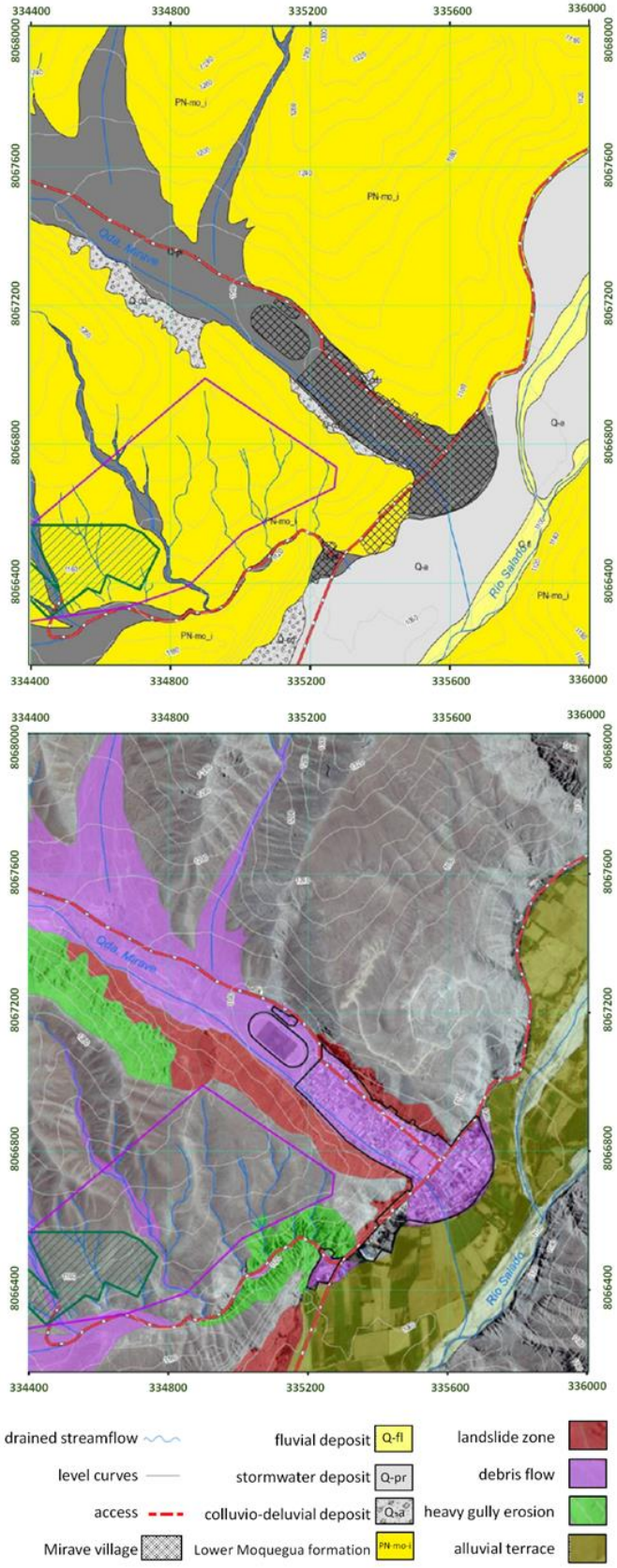

Figure 4. Geological map and geological hazards due to mass movements of Mirave.

The twelve soil sample collection points are shown in Figure 5, along with the location of the town of Mirave in the alluvial fan formed at the mouth of the basin. The geotechnical properties of the soils were evaluated by conducting field and laboratory tests. Altered samples were collected at a depth of 30 cm for moisture tests (ASTM D2216-19, 2020a), Atterberg limits (ASTM D4318-17e1, 2020d), specific gravity tests (ASTM D5550-14, 2020e), grain-size tests (ASTM D6913M-17, 2020f), soil classification (ASTM D2487-17e1, 2020b), and direct shear under drained conditions (ASTM D3080/D3080M-11, 2020c). The direct shear test was performed using particles smaller than 4.8 mm in diameter and with the average density of the soil.

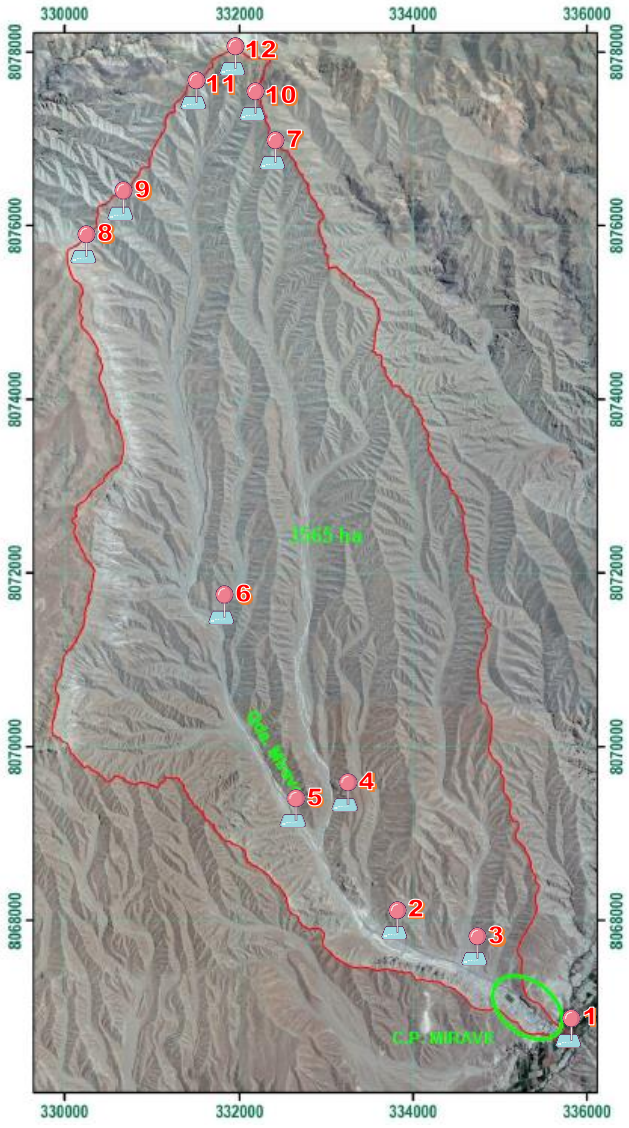

Sampling points:

1	335707.89 m E	8066642.09 m S
2	333850.35 m E	8067677.79 m S
3	334639.54 m E	8067520.66 m S
4	332845.92 m E	8069951.51 m S
5	332273.36 m E	8069779.99 m S
6	331775.86 m E	8071585.78 m S
7	332414.79 m E	8076782.27 m S
8	330062.45 m E	8075712.58 m S
9	330333.20 m E	8075921.82 m S
10	332185.99 m E	8077410.54 m S
11	331586.27 m E	8077599.94 m S
12	332024.01 m E	8077853.18 m S

Figure 5. Delimitation map of the Mirave Micro-basin and sampling points.

3. RESULTS AND DISCUSSION

3.1. Lithological Characteristics

In the area corresponding to the Mirave Sub-basin, four areas with different lithology were observed, corresponding to Paleogene–Neogene sedimentary rocks and Quaternary deposits. These include conglomerates of the upper Moquegua formation, conglomerates of the lower Moquegua formation, andesites of the Paralanque formation, and recent alluvial deposits (sands and gravels). Matrix-supported conglomerates (from the lower Moquegua formation) have

polymictic clasts with subrounded to subangular characteristics and poorly sorted features, with a maximum particle size of 5 cm. These materials are present in the lower basin forming escarpments, especially at the outflow of the drainage. In the middle and upper part, these materials form steeply sloping reliefs with a noticeable presence of colluvial and residual materials. A large number of gullies are concentrated in the primary area, which indicates the erodible characteristics of the materials. Figure 6a shows this type of material located at the headwaters. These materials contain fine whitish particles very similar to volcanic tuffs in some parts of the matrix.

The second lithological area contains clast-supported conglomerates (from the upper Moquegua formation), and it is located in escarpments on the left bank and upper Mirave Basin. These materials are located in the watershed on the right bank of the basin, covering an area of approximately 6 km. They are characterized by their lithic aspect with the presence of poorly sorted subrounded polymictic clasts with an average size of 30 cm; however, they can be as large as 80 cm. In Figure 6b, part of a steep side can be observed with some of these materials. The formation of loose clasts on the slopes is a typical feature. The gullies in these areas present an abrupt initiation followed by a smooth one, with accumulation of larger materials in the natural channels.

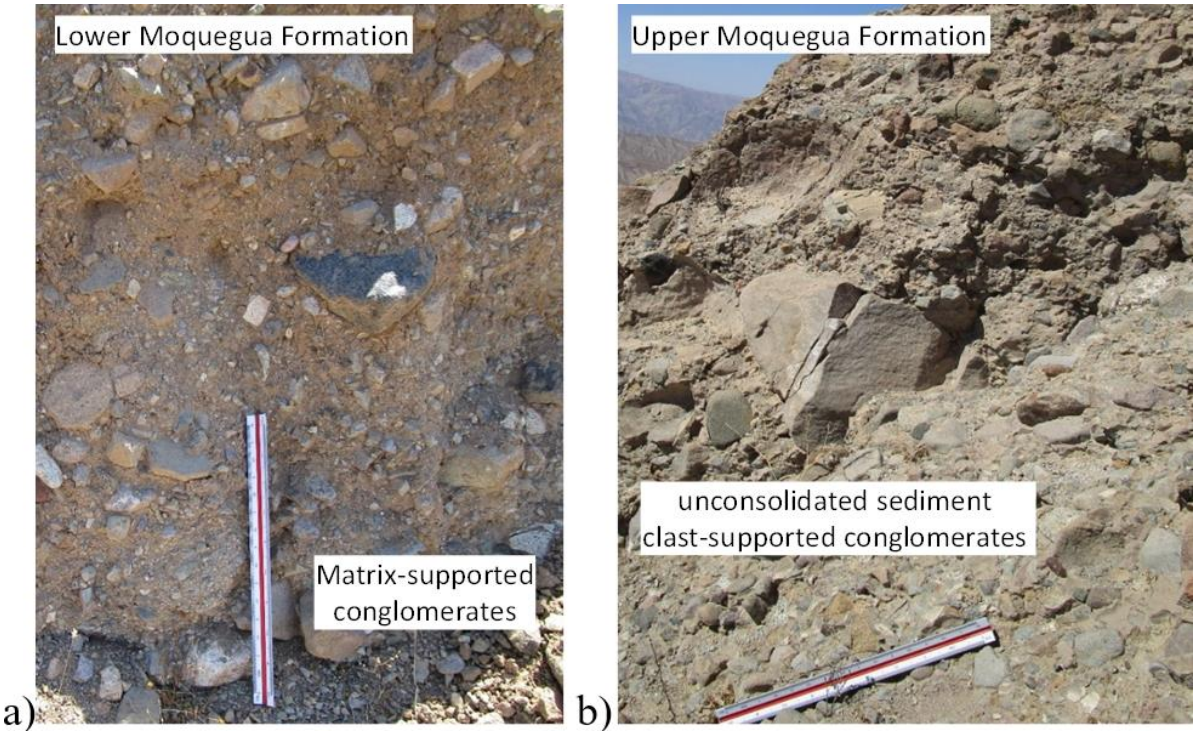

Figure 6. a) Matrix-supported conglomerates and b) clast-supported conglomerates.

The third lithological area contains andesites, which emerge in the left head of the Mirave basin, where the highest point of the basin is located at 2404 masl. The hillsides of these rock formations have an average slope of 30°. Fractured rock massifs and thin layers of soil indicate the action of weathering (Figure 7a). The soils of the hillsides exhibit angular and subangular rock fragments of different sizes (blocks, boulders, cobbles, and gravels). The action of water in this area has resulted in the formation of some small streams that transport the materials contained in the riverbed to the lowest parts. In the 2019 catastrophic event, angular blocks were observed in the Mirave dejection cone, which indicate that they originated in this region. The last lithological area is the alluvial deposits, formed by different debris-flow sediments. Figure 7b shows these deposits that are located in the upper zones. These are characterized by being unconsolidated, and their particles are frequently removed when debris flows are

activated.

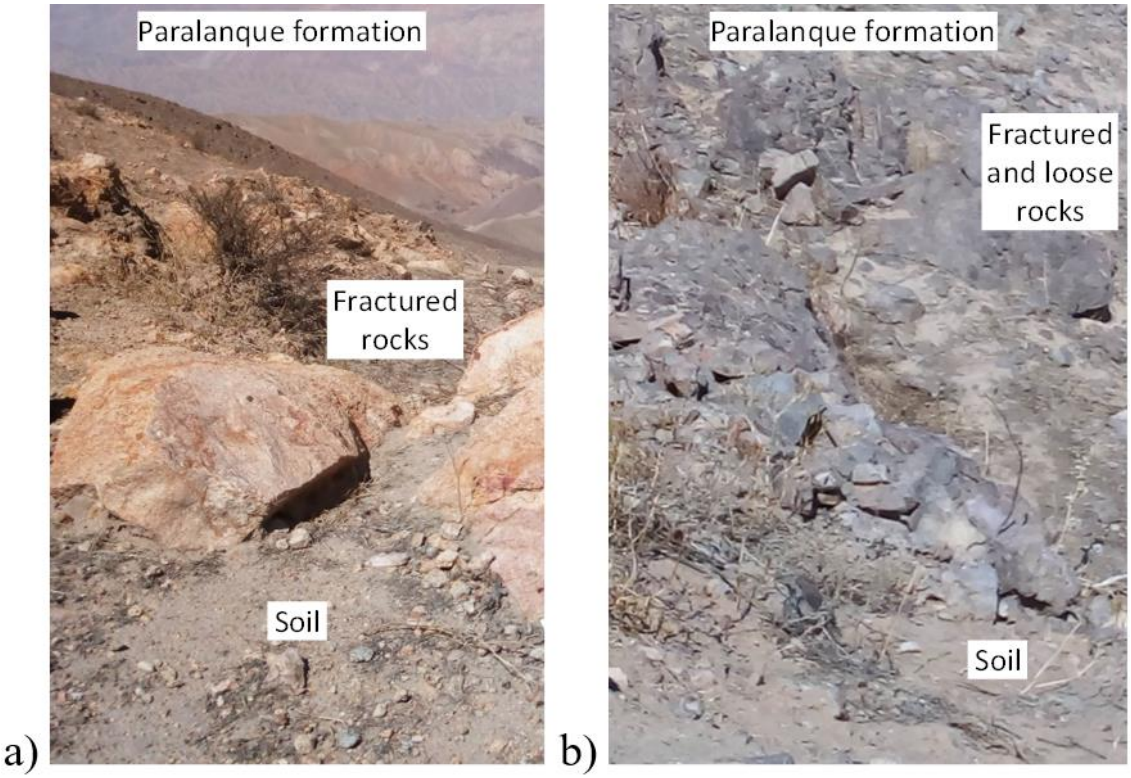

Figure 7. Rock undergoing physical a) alteration and b) weathering.

3.2. Deposit Classification

The samples collected from the field were analyzed by conducting gradation test, Atterberg limit test, specific gravity test, natural moisture content determination, and direct shear test for only one sample. These analyses were performed at the Soils and Rocks Laboratory of the Civil Engineering Department of Universidad de Lima. Undisturbed samples of twelve 30–40-cm deep pits were located at the head of the Mirave Sub-basin, as shown in Figure 5.

The particle-size distribution (or granulometric curve) of the samples obtained through the ASTM D6913/D6913M-17 standard is shown in Figure 8, which presents soil gradation between 75 mm (3 in) and 0.075 mm. Table 1 shows the results of the analyses conducted for the soil samples and presents a detailed summary of the sieving particle analysis. Of the 12 samples tested, 9 are granular soils or silty gravels, which do not present cohesion or plasticity due to the null presence of clay. All the plasticity tests carried out with the ASTM D4318-17e1 standard did not show plasticity, so it can be concluded that the fines present in the sample are all non-plastic silt, which is a type of granular soil, although they have higher fine content such as of 15 or 20%. Sample 1, located in the town of Mirave, non-plastic silt and with 98% fines, it is understood that the majority is silt and there is no clay due to its lack of plasticity. Finally, from the field inspection of the basin and the debris flow event of February 2019 (Del Savio *et al.*, 2019), the classification and characterization of the Mirave Basin is: Morphologically is a debris flows in riverbed; geological structure is an erosion of residual soils and rock weathering; mechanism of occurrence is landslides and accumulation of material in the riverbed; transportation mechanism is highly non-stationary and pulsating; effect on the river bed is erosive and granulometry is coarse granulometry (pebbles, gravel, sands and silts).

According to the granulometric curve of soils, sand and gravel particles can be classified as well or poorly graded. To this end, two parameters were determined: 1) the uniformity coefficient (C_u), which evaluates how evenly the soil granulometry is distributed; and 2) the gradation coefficient (C_c), which evaluates the progression of the variation in the size of the

soil particles (Wibisono *et al.*, 2018). According to ASTM D6913M-17, well-graded sands and gravels must satisfy $C_u \geq 6$ and $C_u \geq 4$, respectively, and $1 \leq C_c \leq 3$; if they do not satisfy any of these criteria, they will be poorly graded. From the lab results of granulometry, C_u was found to vary from 8.9 to 887.7 and C_c ranged from 0.6 to 8, which lead to the conclusion that the evaluated soils are mixed and can be classified between well and poorly graded. Based on the soil plasticity tests (ASTM D4318-17e1, 2020d), the soils were determined to be non-plastic (NP) because of the absence of fine soils (silt or clays) greater than 12% in their composition, which is common in soils without cohesion. The results from the specific gravity of solids (ASTM D5550-14, 2020e) were in the range of 2.65–2.67, which are typical values for sands. The direct shear test (ASTM D3080/D3080M-11, 2020c) was conducted using particles smaller than 4.8 mm in diameter and with an average density of 1.68 g/cm^3, resulting in an average friction angle of 40.4° and cohesion equal to zero.

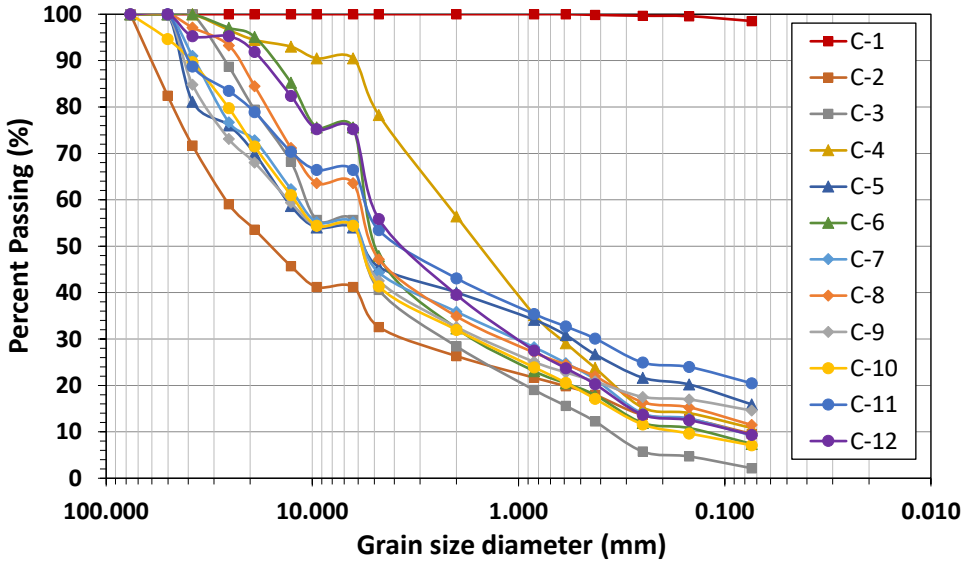

Figure 8. Granulometric curves of samples collected.

The soil erosion factor (K) can be used to measure the susceptibility of soil particles to detachment and transport by surface runoff. For this study, we used the Sharpley and Williams, (1990), *Revised Universal Soil Loss Equation* (RUSLE) concept to determine the soil erosion of the samples brought to the laboratory. The factors affecting erosion are the texture, structure, permeability, and organic content of the soil. Among these factors, texture is the most influential. Several authors use different methods to indirectly determine soil erosion (Renard *et al.*, 1997; Sharpley and Williams, 1990; Wischmeier and Smith, 1978; Hooke, 2003; Romero-Díaz *et al.*, 2007).

For the fraction of sand, silt and clay, in this work used on the Erosion Productivity Impact Calculator - EPIC model (Sharpley and Williams, 1990). The Equation 1 is as follows:

$$K = \left\{0.2 + 0.3exp\left[-0.0256SAN\left(1 - \frac{SIL}{100}\right)\right]\right\} x \left(\frac{SIL}{CLA+SIL}\right)^{0.3} x \left[1 - \frac{0.25C'}{C'+exp(3.72-2.95C')}\right] x \left[1 - \frac{0.7SN_1}{SN_1+exp(-5.51+22.9SN_1)}\right] \quad (1)$$

Where *SAN* is the sand fraction in %; *SIL* is the silt fraction in %; *CLA* is the clay fraction in %; *C'* is the soil total organic carbon content in %; and SN_1=1-*SAN*/100.

Then, to find the modified K value considering the gravel fraction as a key parameter, the proposal by Chang-Xing (2009) and used in works such as Wang *et al.*, 2013 and Hu *et al.* 2019, to modify soil erodibility for different ranges of gravel content. The modification

coefficient M (relative soil erosion) was determined by the following Equation 2:

$$M = \{0.0781exp(-0.0249G)\ 0.294 - 0.0123G\ 1 - 0.0829G\ G > 20\%\ 10\% < G \leq 20\%\ G \leq 10\% \quad (2)$$

Where G is the gravel content. The modified soil erodibility (K_r) can be calculated by the following Equation 3:

$$K_r = K \cdot M \quad (3)$$

As explained above, in the 12 samples silt predominates over clay; therefore, assuming that the clay content is 10% of the fines, the values of K and Kr presented in Table 1 were calculated. It can be seen that the Kr range increases notably with values of 0.48 and 1.12, as minimum and maximum respectively. This indicates the important effect of gravel content in the calculation of soil erosion. Considering that the silt content is greater than the clay content, Kr values greater than 0.4 will be obtained, which indicates that they are the most erodible of all soils. This means that they separate easily and tend to form high runoff rates. Finally, the annual soil losses in the study area show that the erosion factor is high.

From the soil analysis, it was found that the soil has a high content of non-plastic silt (they do not have enough colloids) and results in an area susceptible to erosion. The unconsolidated conglomerate of the formation presents an unstable sandy-silty matrix favoring an increase in the production of loose materials. Therefore, it was quantified that the erosion processes of all the slopes adjoining the channel of the stream generate loose material that, in the event of extraordinary rains, is dragged into the channel. Finally, the study will continue to take into consideration the information from the rain gauge recently installed in Mirave, in order to have a better understanding of the triggering factors of flows and slope erosion.

3.3. Discussion

Fine soils or particles smaller than 0.005 mm with an IP of less than 4 do not have sufficient colloids to support erosion (Grabowski *et al.*, 2011; Grissinger, 1966; Sherard *et al.*, 1976; Smerdon and Beasley, 1959; Lyle and Smerdon, 1965). Briaud *et al.* (2017) reported that SP materials (poorly graded sand), SM (silty sand), and ML (low plasticity silt) exhibit obvious erosional features. Therefore, the presence of NP silts in the matrix of the soils under analysis in this study may be related to the areas susceptible to erosion. The latter does not mean that plastic materials do not undergo erosion, because, as mentioned by Partheniades (2006), a plastic clay can be easily eroded under moving water depending on the water chemistry.

Areas with erosional evidence linked to debris flows in the studied region show that materials with variable percentages of sand and silt ranging from 40% to 55% and without plasticity are susceptible to erosional processes. Surface hydraulic erosion processes act with greater intensity on materials without plasticity and with particles between 0.01 and 1-mm diameter (Yang and Liu, 2016); i.e., silts and sands. The matrix-supported conglomerates, which are predominant in the Mirave Sub-basin, exhibit an unstable sandy-silt matrix when undergoing erosional processes. The instability of the matrix disintegrates the unconsolidated conglomerate of the Moquegua formation, favoring an increase in the production of loose materials. The loose materials of the hillside, the loose materials in the gullies, and the disaggregated materials from previous landslides are usually the result of the debris flows (Brayshaw and Hassan, 2009; Glade, 2005; Takahashi, 2009). These processes occur at the head of the Mirave Micro Basin with a higher intensity, which is similar to what has been recorded in other studies (Brayshaw and Hassan, 2009; Jakob, 2005).

Three profiles with different lithology are analyzed in Figure 9 to discuss how lithological features affect the generation of different types of debris flows, all located in the headwaters of the Mirave Micro Basin.

Table 1. Report of tests analysis for samples.

ID	USCS	w (%)	G_s	%G	%S	%F	LL	PL	D_{10} (mm)	D_{30} (mm)	D_{60} (mm)	C_U	C_C	K	K_r
C-1	ML	5.7	-	0.0	1.5	98.5	NP	NP	0.002	-	-	-	-	0.483	0.483
C-2	GP-GM	1.5	2.65	67.4	23.0	9.5	NP	NP	0.082	3.327	26.184	320.5	5.2	0.363	0.530
C-3	GW	2.1	-	59.4	38.4	2.2	NP	NP	0.355	2.240	10.520	29.7	1.3	0.305	0.542
C-4	SP-SM	1.5	-	21.7	67.4	10.8	NP	NP	0.054	0.622	2.304	43.0	3.1	0.247	1.124
C-5	GM	1.4	-	54.5	29.6	15.9	NP	NP	0.015	0.552	13.309	888.7	1.5	0.346	0.695
C-6	GP-GM	1.1	-	52.1	40.5	7.4	NP	NP	0.126	1.613	5.399	42.8	3.8	0.304	0.649
C-7	GW-GM	1.8	2.64	55.7	35.1	9.2	NP	NP	0.086	1.028	11.577	134.1	1.1	0.321	0.627
C-8	GP-GM	3.2	-	52.8	35.7	11.5	NP	NP	0.043	1.162	5.961	139.7	5.3	0.322	0.675
C-9	GM	1.2	-	57.5	28.0	14.6	NP	NP	0.019	1.483	13.069	682.5	8.8	0.350	0.653
C-10	GW-GM	1.5	2.66	58.7	34.2	7.1	NP	NP	0.164	1.620	12.143	74.2	1.3	0.322	0.583
C-11	GM	2	-	46.5	33.0	20.5	NP	NP	0.008	0.421	5.504	671.1	3.9	0.340	0.832
C-12	SW-SM	1.1	-	44.1	46.5	9.3	NP	NP	0.086	1.005	5.062	59.2	2.3	0.291	0.758

USCS: Unified Soil Classification System; w: water content: Gs: specific gravity of soils; LL, PL: Liquid and Plastic Limit; %G, %S, %F: Gravel, Sand and Fine content; Dx: x% of the soil particles are finer than this size; Cu; uniformity coefficient; Cc: coefficient of curvature; K: soil erodibility factor; K_r: modified soil erodibility

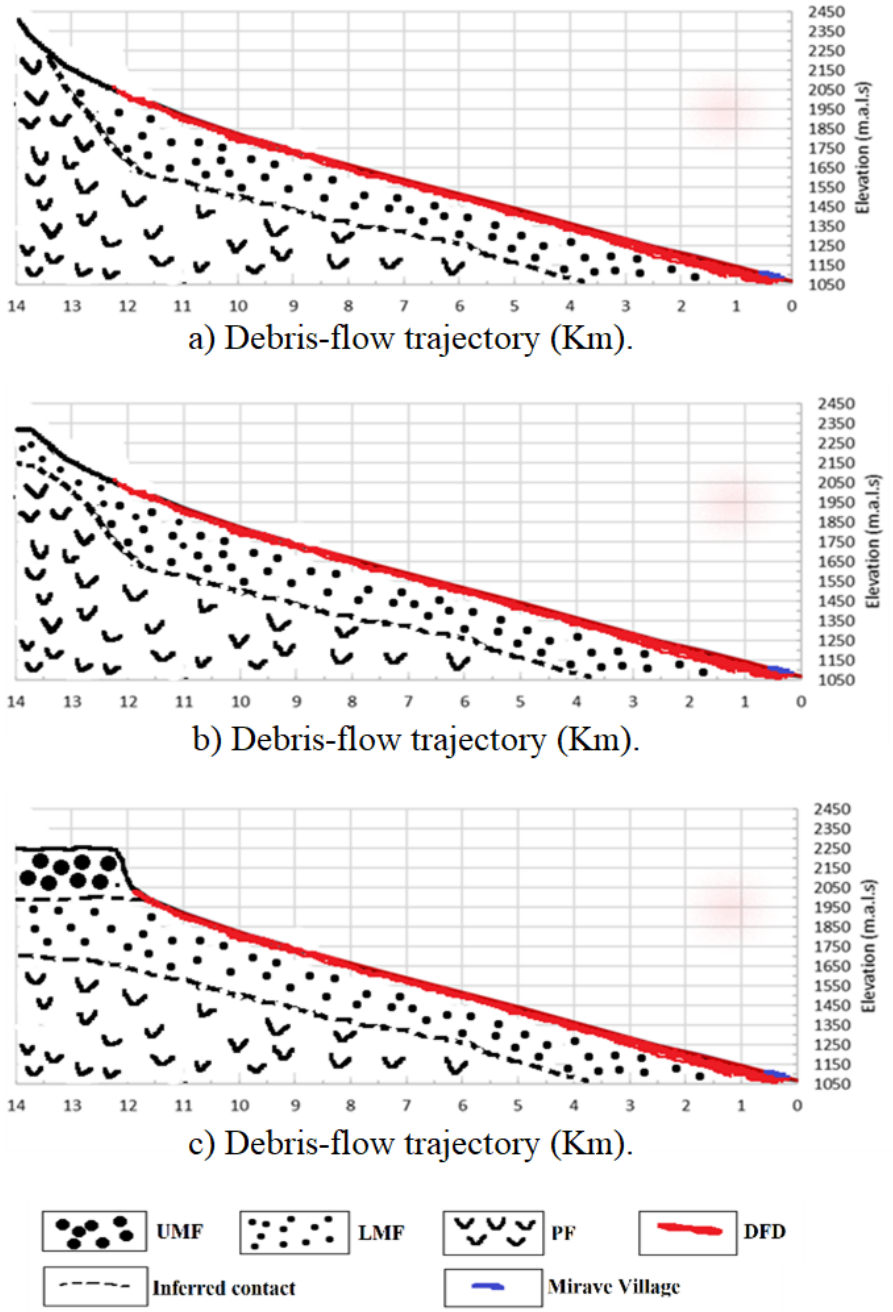

Figure 9. a) Andesite head; b) supported array conglomerate head; and c) head of supported clast conglomerates.

The first one occurs in areas of rocky outcrops of volcanic origin (Figure 9a), where the debris flow is generated by the action of water concentrated in furrows, which, because of the high slopes of these formations, is strong enough to transport angular debris contained in its course to the lower parts. In the field study conducted after the 2019 event, it was found that the blocks have angular shapes, a material that comes from the Mirave dejection. The transport of angular rock type blocks required a greater hydraulic energy in the form of water courses for their movement, which indicates that they may be related to large events, such as the one that took place in 2019. Downstream flows down the rills at high speed may contribute to the generation of debris flows downstream, specifically in the gully channel in which loose sediments are accumulated.

The matrix-supported conglomerates of the lower Moquegua formation exhibit irregular

distributions and contain polymictic clasts. Two types of these materials can be identified with different erosive behavior in terms of water (Figure 9b). Water erosion in these materials has formed numerous gullies, with different depths and extensions and without the presence of a water table. These gullies are distributed throughout most of the basin. The interior of the gullies shows intense erosive activity and accumulation of materials transported by gravity and water. The advance of the gullies in the upper Mirave Basin affects hillsides with steep slopes (approximately 30°), causing potential landslides at the contact of the gully and the hillside, which can lead to the onset of debris flows. The surface soils of approximately 20-cm diameter cover the slopes that are unaffected by the gullies and present vegetation only in the summer months (January, February, and March).

The lithological unit comprises nonuniform consolidated and clast-supported conglomerates of the upper Moquegua formation (Figure 9c). Physical weathering acts slowly to disaggregate the conglomerate clasts, and environmental agents transport these loose materials down the hillside. They can be accumulated on the hillsides and in the channels of pre-existing gullies of the lower Moquegua formation, which exhibit a more moderate relief. High speed streams fall as jets or small waterfalls onto the lower areas and are connected to different creeks. With that energy, they enter the areas of colluvial materials and in some cases (especially when the force of the water is strong, such as in big storms), can liquefy these materials and initiate the flow of debris.

4. CONCLUSIONS

Given the arid climate of the Mirave region, the formation of clay surface soils is not typical. The low percentage of this type of minerals indicates low cohesion; thus, the matrix-supported conglomerates and their corresponding residual and colluvial soils are in advanced erosion processes. The erosion of the matrix of these conglomerates causes the collapse of these materials, which are the most abundant in the debris flow generating zones of the Mirave Sub-basin. At the headwaters, a change in sediment production has been found, primarily generated from residual and colluvial soils, enhancing the debris flow generation mechanism.

The main geotechnical features in these arid mountain basins are particle size, plasticity, and erodibility. The absence of plasticity and the abundance of potentially erodible particles because of their size (sand and silt) strengthen the erosive features of the region, i.e., the abundance of gullies and rills. However, to quantify erosion, future studies should conduct rock tests, in addition to considering the use of methodologies for calculating the erosion factor according to taxonomic classes, with a greater number of samples that allow for a stricter statistical analysis.

In this study, the evaluation of the source of debris flows in the Mirave Basin has identified that erosion processes on hillsides maximize geologic hazards and risks to human communities established in the alluvial fan of the basin.

5. ACKNOWLEDGMENTS

This research was supported by the National Innovation Program for Competitiveness and Productivity (Innóvate Perú) of the Ministry of Production of Peru and the Scientific Research Institute (IDIC) of the Universidad de Lima with Project Number 687-INNOVATEPERU-RPR-2017.

6. REFERENCES

ASTM INTERNATIONAL. **ASTM D2216-19**. Standard Test Methods for Laboratory Determination of Water (Moisture) Content of Soil and Rock by Mass. West Conshohocken, 2020a.

ASTM INTERNATIONAL. **ASTM D2487-17e1**. Standard Practice for Classification of Soils for Engineering Purposes (Unified Soil Classification System). West Conshohocken, 2020b.

ASTM INTERNATIONAL. **ASTM D3080/D3080M-11**. Standard Test Method for Direct Shear Test of Soils Under Consolidated Drained Conditions. West Conshohocken, 2020c.

ASTM INTERNATIONAL. **ASTM D4318-17e1.** Standard Test Method for Specific Gravity of Soil Solids by Gas Pycnometer. West Conshohocken, 2020d.

ASTM INTERNATIONAL. **ASTM D5550-14.** Standard Test Methods for Liquid Limit, Plastic Limit, and Plasticity Index of Soils. West Conshohocken, 2020e.

ASTM INTERNATIONAL. **ASTM D6913M-17**. Standard Test Methods for Particle-Size Distribution (Gradation) of Soils Using Sieve Analysis. West Conshohocken, 2020f.

BELLIDO BRAVO, E. **Geology of the Moquegua Quadrangle. Page: 35-u**. Lima: Instituto Geológico Minero y Metalúrgico, 1979.

BRAYSHAW, D.; HASSAN, M. A. Debris flow initiation and sediment recharge in gullies. **Geomorphology**, v. 109, n. 3-4, p. 122-131, 2009. https://doi.org/10.1016/j.geomorph.2009.02.021

BRIAUD, J.-L.; GOVINDASAMY, A. V.; SHAFII, I. Erosion charts for selected geomaterials. **Journal of Geotechnical and Geoenvironmental Engineering**, v. 143, n. 10, p. 04017072, 2017. https://ascelibrary.org/doi/full/10.1061/(ASCE)GT.1943-5606.0001771

CANNON, S. H.; RENEAU, S. L. Conditions for generation of fire-related debris flows, Capulin Canyon, New Mexico. **Earth Surface Processes and Landforms**, v. 25, n. 10, p. 1103-1121, 2000. https://doi.org/10.1002/1096-9837(200009)25:10%3C1103::AID-ESP120%3E3.0.CO;2-H

CHANG, M.; LIU, Y.; ZHOU, C.; CHE, H. Hazard assessment of a catastrophic mine waste debris flow of Hou Gully, Shimian, China. **Engineering Geology**, v. 275, p. 105733, 2020. https://doi.org/10.1016/j.enggeo.2020.105733

CHANG-XING, S. H. I. Effects of gravel content on soil erodibility and the methods of estimating soil erodibility factor K. **Chinese Journal of Soil Science,** v. 40, n. 6, p. 1398–1401, 2009.

CHEN, J.-C.; LIN, C.-W.; WANG, L.-C. Geomorphic characteristics of hillslope and channelized debris flows: A case study in the Shitou area of central Taiwan. **Journal of Mountain Science**, v. 6, n. 3, p. 266-273, 2009. https://doi.org/10.1007/s11629-009-0250-0

DECOU, A.; VON EYNATTEN, H.; DUNKL, I.; FREI, D.; WÖRNER, G. Late Eocene to Early Miocene Andean uplift inferred from detrital zircon fission track and U–Pb dating of Cenozoic forearc sediments (15-18°S). **Journal of South American Earth Sciences**, v. 45, p. 6-23, 2013. https://doi.org/10.1016/j.jsames.2013.02.003

DEL SAVIO, A. A.; QUISCA ASTOCAHUANA, S. I.; CASTILLO NAVARRO, L. F. Numerical simulation of debris flows of the catastrophic event of February 2019 in Mirave–Peru. **Revista Ambiente & Água**, v. 14, n. 6, p. 1-20, 2019. https://doi.org/10.4136/ambi-agua.2437

DI, B.; ZHANG, H.; LIU, Y. *et al.* Assessing susceptibility of debris flow in Southwest China using gradient boosting machine. **Scientific Reports**, v. 9, n. 1, p. 12532, 2019. https://doi.org/10.1038/s41598-019-48986-5

DING, M.; HUANG, T.; ZHENG, H.; YANG, G. Respective influence of vertical mountain differentiation on debris flow occurrence in the Upper Min River, China. **Scientific Reports**, v. 10, n. 1, p. 11689, 2020. https://doi.org/10.1038/s41598-019-48986-5

ESPER ANGILLIERI, M. Y. Debris flow susceptibility mapping using frequency ratio and seed cells, in a portion of a mountain international route, Dry Central Andes of Argentina. **CATENA**, v. 189, p. 104504, 2020. https://doi.org/10.1016/j.catena.2020.104504

ESPER ANGILLIERI, M. Y.; PERUCCA, L.; VARGAS, N. Spatial and temporal analysis of debris flow occurrence in three adjacent basins of the western margin of Grande River: Quebrada de Humahuaca, Jujuy, Argentina. **Geografiska Annaler: Series A, Physical Geography**, v. 102, n. 2, p. 83-103, 2020. https://doi.org/10.1080/04353676.2020.1744075

GLADE, T. Linking debris-flow hazard assessments with geomorphology. **Geomorphology**, v. 66, n. 1-4, p. 189-213, 2005. https://doi.org/10.1016/j.geomorph.2004.09.023

GRABOWSKI, R. C.; DROPPO, I. G.; WHARTON, G. Erodibility of cohesive sediment: The importance of sediment properties. **Earth-Science Reviews**, v. 105, n. 3-, p. 101-120, 2011. https://doi.org/10.1016/j.earscirev.2011.01.008

GRISSINGER, E. H. Resistance of selected clay systems to erosion by water. **Water Resources Research**, v. 2, n. 1, p. 131-138, 1966. https://doi.org/10.1029/WR002i001p00131

GUERRERO, P. C.; ROSAS, M.; ARROYO, M. T. K.; WIENS, J. J. Evolutionary lag times and recent origin of the biota of an ancient desert (Atacama-Sechura). **Proceedings of the National Academy of Sciences of the United States of America**, v. 110, n. 28, p. 11469-11474, 2013. https://doi.org/10.1073/pnas.1308721110

HOOKE, J. Coarse sediment connectivity in river channel systems: a conceptual framework and methodology. **Geomorphology**, v. 56, n. 1-2, p. 79-94, 2003. https://doi.org/10.1016/S0169-555X(03)00047-3

HOUSTON, J. Variability of precipitation in the Atacama Desert: its causes and hydrological impact. **International Journal of Climatology**, v. 26, n. 15, p. 2181-2198, 2006. https://doi.org/10.1002/joc.1359

HU, S.; LI, L.; CHEN, L.; CHENG, L.; YUAN, L.; HUANG, X. *et al.* Estimation of Soil Erosion in the Chaohu Lake Basin through Modified Soil Erodibility Combined with Gravel Content in the RUSLE Model. **Water**, v. 11, n. 9, p. 1806, 2019. https://doi.org/10.3390/w11091806

HUNGR, O. Classification and terminology. **Debris-flow Hazards and Related Phenomena**. p. 9-23, 2005. Berlin: Springer Praxis Books.

ILABAYA. District Municipality. **Risk assessment report on debris flow risk in the town of Mirave, district of Ilabaya, province of Jorge Basadre, Tacna Department.** Lima: Centro Nacional d Estimación, Prevención y Reducción del Riesgo de Desastres, 2016.

IMAIZUMI, F.; TSUCHIYA, S.; OHSAKA, O. Behavior of boulders within a debris flow initiation zone. **International Journal of Erosion Control Engineering**, v. 9, n. 3, p. 91-100, 2016. https://doi.org/10.13101/ijece.9.91

INDECI. **Complementary Report Number 408 - 09/02/2019/COEN - INDECI/02:20 Hours (Report N° 01) Huaico en el distrito de Ilabaya–Tacna**. 2019. Available: https://www.indeci.gob.pe/emergencias/tacna-jorge-basadre-ilabaya-mirave-huaico-reporte-complementario-01 Access: 8 Aug. 2020.

JAKOB, M. A size classification for debris flows. **Engineering Geology**, v. 79, n. 3-4, p. 151-161, 2005. https://doi.org/10.1016/j.enggeo.2005.01.006

LARA, G.; PERUCCA, L.; ROTHIS, M. Morphometric, geomorphologic and flood hazard analysis of an arid mountain river basin, central pre-Andes of Argentina. Southwestern South America. **Geografia Fisica e Dinamica Quaternaria, GFDQ**, v. 41. p. 83-97, 2018

LYLE, W. M.; SMERDON, E. T. Relation of compaction and other soil properties to erosion resistance of soils. **Transactions of the ASAE**, v. 8, n. 3, p. 419-422, 1965. https://doi.org/10.13031/2013.40536

MARTINEZ, W.; ZULOAGA, A. **Explanatory Report of the geology of the Moquegua Quadrangle. (35-u)**. 2000. Available: https://repositorio.ingemmet.gob.pe/handle/20.500.12544/2044. Access: 5 June 2021.

MEDINA ALLCA, L.; LUQUE POMA, G. **Evaluation of geological hazards in Mirave town center and Alto Mirave sector.** Lima: INGEMMET, 2016.

MELÉNDEZ, D.; RAMOS-FERNÁNDEZ, L.; VELÁSQUEZ, T.; ALTAMIRANO, L. Simulation with a conceptual distributed hydrological model on a daily scale in a semi-arid basin of the Lurin River, Peru. **Idesia,** v. 39, n. 1, 2021.

MEYER, N. K.; SCHWANGHART, W.; KORUP, O.; NADIM, F. Roads at risk–traffic detours from debris flows in southern Norway. **Natural Hazards and Earth System Sciences Discussions**, v. 2, p. 6623-6651, 2014. https://doi.org/10.5194/nhess-15-985-2015

MOREIRAS, S. M. Frequency of debris flows and rockfall along the Mendoza river valley (Central Andes), Argentina: Associated risk and future scenario. **Quaternary International**, v. 158, n. 1, p. 110-121, 2006. https://doi.org/10.1016/j.quaint.2006.05.028

MOREIRAS, S. M.; SEPÚLVEDA, S. A.; CORREAS-GONZÁLEZ, M.; LAURO, C.; VERGARA, I.; JEANNERET, P. *et al*. Debris Flows Occurrence in the Semiarid Central Andes under Climate Change Scenario. **Geosciences,** v. 11, 43, 2021. https://doi.org/10.3390/geosciences11020043

PARTHENIADES, E. **Engineering properties and hydraulic behavior of cohesive sediments**. Boca Raton: CRC Press, 2006.

RENARD, K. G.; FOSTER, G. R.; WEESIES, G. A.; MCCOOL, D. K.; YODER, D. C. **Predicting soil erosion by water: a guide to conservation planning with the Revised Universal Soil Loss Equation (RUSLE)**. Washington, D.C.: U.S. Dept. of Agriculture, 1997.

ROMERO-DÍAZ, A.; ALONSO-SARRIÁ, F.; MARTÍNEZ-LLORIS, M. Erosion rates obtained from check-dam sedimentation (SE Spain). A multi-method comparison. **CATENA**, v. 71, n. 1, p. 172-178, 2007. https://doi.org/10.1016/j.catena.2006.05.011

SENAMHI. **National hydrometeorological data**. Available: https://www.senamhi.gob.pe/servicios/?p=estaciones. Access: 7 July 2021.

SHARPLEY, A. N.; WILLIAMS, J. R. (Orgs.). **EPIC, Erosion/Productivity Impact Calculator. 1, Model documentation**. Springfield: Agricultural Research Service, 1990.

SHERARD, J. L.; DUNNIGAN, L. P.; DECKER, R. S. Identification and nature of dispersive soils. **Journal of the Geotechnical Engineering Division**, v. 102, n. 4, p. 287-301, 1976. https://doi.org/10.1061/AJGEB6.0000256

SMERDON, E. T.; BEASLEY, R. P. **The tractive force theory applied to stability of open channels in cohesive soils**. Columbia: University of Missouri, College of Agriculture, 1959. p. 1-36.

STOLLE, A.; LANGER, M.; BLÖTHE, J. H.; KORUP, O. On predicting debris flows in arid mountain belts. **Global and Planetary Change**, v. 126, p. 1-13, 2015. https://doi.org/10.1016/j.gloplacha.2014.12.005

TAKAHASHI, T. A review of Japanese debris flow research. **International Journal of Erosion Control Engineering**, v. 2, n. 1, p. 1-14, 2009. https://doi.org/10.13101/ijece.2.1

WANG, B.; ZHENG, F.; RÖMKENS, M. Comparison of soil erodibility factors in USLE, RUSLE2, EPIC and Dg models based on a Chinese soil erodibility database. **Acta Agriculturae Scandinavica, Section B — Soil & Plant Science**, v. 63, n. 1, p. 69-79, 2013. https://doi.org/10.1080/09064710.2012.718358

WIBISONO, G.; NUGROHO, S. A.; UMAM, K. The influence of sand's gradation and clay content of direct shear test on clayey sand. **IOP Conference Series: Materials Science and Engineering**, v. 316, p. 012038, 2018.

WISCHMEIER, W. H.; SMITH, D. D. **Predicting rainfall erosion losses: a guide to conservation planning**. Washington, D.C.: U.S. Dept. of Agriculture, 1978.

YANG, J.; LIU, X. Shear wave velocity and stiffness of sand: the role of non-plastic fines. **Géotechnique**, v. 66, n. 6, p. 500-514, 2016. https://doi.org/10.1680/jgeot.15.P.205